Process Biochemistry 156 (2025) 308–316

Contents lists available at ScienceDirect

Process Biochemistry

journal homepage: www.elsevier.com/locate/procbio

Fast and green process to obtain astaxanthin-rich extracts from shrimp shell waste for dye sensitized solar cells

Francesco Milano [a], Federica Mancarella [b], Livia Giotta [b], Ilaria Citro [c,*], Stefano Trocino [d], Giuseppe Calogero [c], Donatella Spadaro [c]

[a] Institute of sciences of food production (ISPA)- National Research Council – Lecce, SP Lecce-Monteroni, 73100 Lecce, Italy
[b] Department of biological and environmental sciences and technology (DISTEBA) University of Salento, SP Lecce-Monteroni, 73100 Lecce, Italy
[c] Institute for Chemical and Physical Processes (IPCF)- National Research Council - Messina, Viale Ferdinando Stagno d'Alcontres, n. 37, 98158 Messina, Italy
[d] Institute for Advanced Energy Technologies "Nicola Giordano" (ITAE) - National Research Council (CNR), Via Salita S. Lucia sopra Contesse, n. 5, 98126 Messina, Italy

ARTICLE INFO

Keywords:
DSSC
Natural dyes
Carotenoid
Xanthophyll
De-esterification

ABSTRACT

Aiming to address the critical need for renewable energy, this study explores the potential of astaxanthin-rich extracts from shrimp waste as natural sensitizers for dye-sensitized solar cells (DSSCs) using an eco-friendly and economically viable process. Photoconversion efficiencies (PCE) of astaxanthin-based DSSCs were evaluated through I-V measurements while charge transfer resistances (R_{CT}) were assessed by electrochemical impedance spectroscopy. The sensitizer preparation involved extraction of astaxanthin from waste shrimp (*Aristaeomorpha foliacea*) cephalothoraxes, which were desiccated, finely milled and treated with ethyl acetate, to obtain a crude extract very rich in astaxanthin mainly present in esterified forms. The extraction process was fast and avoided extreme experimental conditions in terms of energy consumption, ultra-vacuum, high temperatures and use of toxic solvents. Direct application of the crude extract as sensitizer for DSSCs resulted in low PCE (0.09 %) and high R_{CT}, due to the limited ability of esterified astaxanthin to interact with the TiO_2 layer. This limitation was overcome through saponification of the extract with methanolic NaOH, leading to free astaxanthin with high recovery yield and limited degradation. The saponified extract showed lower R_{CT} and higher PCE (0.30 %). These results highlight the promising potential of suitably processed shrimp waste as a source of sensitizers for DSSCs.

1. Introduction

Global dependence on fossil fuels such as coal, natural gas, and petroleum has led to significant environmental, economic, and geopolitical challenges. These non-renewable resources are undergoing rapid depletion and their extraction, transportation, and consumption significantly contribute to air, water, and soil pollution, as well as to global warming through the emission of greenhouse gases [1,2]. The transition to renewable energy is essential to mitigate climate change, enhance energy security and promote sustainable development. Sources such as solar, wind, hydro, and biomass represent viable alternatives to fossil fuels, as they are abundant, environmentally sustainable, and, if effectively deployed, capable of meeting global energy demands. Furthermore, recent technological advancements have improved their cost-effectiveness, making them more accessible and economically competitive.

Among the various technologies being explored, Dye-Sensitized Solar Cells (DSSCs) have emerged as a promising, low-cost alternative to conventional silicon-based photovoltaic devices. DSSCs offer several advantages, including ease of fabrication, flexibility, and tunable optical properties, such as color and transparency [3].

Typically, synthetic inorganic compounds such as ruthenium(II) complexes with different ligands are used as molecular sensitizers in DSSCs [4,5]. Recent advancements in DSSC technology have focused on improving the efficiency and stability of these cells. For instance, the development of novel dye structures, such as the donor-π-bridge-acceptor (D-π-A) motif, has significantly enhanced light-harvesting capabilities and electron injection efficiency leading to overall photovoltaic efficiencies η greater than 10 %[6].

To replace the rare and expensive ruthenium compounds, numerous

* Corresponding author.
E-mail address: ilaria.citro@cnr.it (I. Citro).

https://doi.org/10.1016/j.procbio.2025.06.006
Received 26 February 2025; Received in revised form 9 June 2025; Accepted 11 June 2025
Available online 16 June 2025

synthetic organic dyes have been extensively researched and tested as cost-effective alternatives with high efficiency values [7]. Other research groups have achieved good solar energy conversion efficiencies, not dramatically lower than those achieved with synthetic dyes, by testing natural dyes as alternative sensitizers, a possibility representing one of the principal advantages of DSSCs [8–10]. Indeed, many natural dyes possess the right characteristics to properly act as sensitizers, such as good absorption in the visible range, suitable HOMO and LUMO energy levels and ability to bind to the TiO_2 semiconducting layer. Such dyes are present in nature as pigments in various fruits, flowers, leaves, and bacteria conferring them their characteristic colors and are widely available, easy to prepare, low-cost, non-toxic, environmentally friendly, and fully biodegradable [11]. The resulting natural pigment-sensitized DSSCs can be used for educational purposes or indoor applications [12]. Additionally, the use of co-sensitization, where multiple natural dyes with complementary absorption spectra are employed, has been shown to increase the overall power conversion efficiency by broadening the range of absorbed wavelengths [13–15].

Recently, several studies have been conducted on the use of pigments extracted from microorganisms in the development of DSSCs [16–18]. These microorganisms exhibit rapid growth and can be cultivated year-round in bioreactors, unaffected by seasonal changes. The pigments produced are typically non-toxic, non-carcinogenic, and biodegradable and are often blends of related compounds, that vary according to the microorganism strain, allowing them to absorb a broad spectrum of light energy, thus influencing the performance of the final devices. Furthermore, the composition of these pigment mixtures can be adjusted by altering cultivation conditions, offering control over the primary pigments produced [19–21]. Examples of natural molecules used as DSSC sensitizers and their corresponding typical efficiencies (η) include chlorophylls (2.6 % [22]), anthocyanins (0.56 %, [23] and 2.61 % using Cu-doped TiO_2, [24]), betalains (2.7 % [25]) and carotenoids (1.0 % [26]). Several other examples have been recently reviewed by Prajapat *et al.* [27]. The versatility and abundance of these natural dyes make them viable options for large-scale applications, particularly in regions with high solar radiation and significant agricultural waste production. Indeed, the possibility of obtaining natural pigments from agri-food materials and waste, represents a compelling opportunity in the context of the circular economy [28,29].

Among natural pigments, astaxanthin (3,3′-Dihydroxy-β,β-carotene-4,4-dione, AST), a xanthophyll-type carotenoid, is a lipid-soluble red-orange pigment, bearing a keto and a hydroxyl group at the cyclic ends of the isoprenoid chain. It is derived from marine algae such as *Haematococcus pluvialis,* and is widely studied due to its numerous beneficial properties in the fields of food, cosmetics [30] and medicine, including anti-inflammatory and insulin-sensitizing effects [31].

Interesingly, AST represents also a promising candidate as a sensitizer for DSSCs since it absorbs light in the visible spectrum, has the proper HOMO and LUMO levels and is able to efficiently bind to the TiO_2 layer. In a recent study, astaxanthin extracted from the microalga *Haematococcus pluvialis*, the yeast *Phaffia rhodozyma*, and the bacterium *Paracoccus carotinifaciens* was used to sensitize DSSCs to evaluate how structural differences influence the dyes' photoelectrochemical behavior [32].

In the context of the circular economy, among the various possible sources of astaxanthin, shrimp waste is one of the most potentially profitable since it is extensively produced in many coastal areas resulting in disposal problems. The shrimp shell waste are particularly rich in astaxanthin [33] and are an important source of further valuable biomaterials like chitin [34], PUFA (including omega-3 fatty acids) [35] and proteins [36]. The multiple products achievable from waste treatment thus increase the efficiency and cost-effectiveness of the biorefining process [37].

In this paper, we therefore explore, for the first time to the best of the author's knowledge, the potential of astaxanthin extracted from shrimp waste to generate renewable energy using DSSCs through an environmentally friendly and economically viable approach. With this purpose, as an additional novel aspect, purification and pigment manipulations were reduced to a very simple and cost-effective process: the shrimp waste, composed of the cephalothoraxes obtained from a local fishing industry, was desiccated, milled to a fine powder and treated at room temperature for a limited time interval with ethyl acetate to obtain a crude AST-rich extract. It is worthwhile to mention that the use of toxic solvents like acetone, hexane or petroleum ether is frequently reported in literature; other methods involve the use of supercritical CO_2, ultrasounds, enzymatic pretreatments, high temperatures or longer incubation times, increasing the costs of production (for a list of extraction methods and relevant yields see Mancarella et al. [38]). When this crude extract was directly used as DSSC sensitizer, a low photoconversion efficiency, compared to AST standard used as reference, was observed. This result was somewhat expected since it is known that AST is mainly present in mono- and diester forms, attached to mono and (poly)--unsaturated fatty acids of various lengths, impairing proper attachment onto the TiO_2 semiconducting layer. Therefore, we applied, as the final novel step, an optimized de-esterification procedure that led to AST with free hydroxyl groups with high yield and negligible degradation as demonstrated by HPLC measurements. The resulting improved photoconversion efficiency from 0.09 % to 0.30 %, comparable to that of the AST standard, was therefore attributed to the presence of free hydroxyl groups that, being in ortho position relative to the keto groups, enable the formation of strong bidentate complexes with the TiO_2 layer. The results obtained using this protocol are therefore very promising and provide a foundation for further studies aimed at investigating the photodegradation of the pigment and the long-term stability of the devices.

2. Materials and methods

2.1. Chemicals

Synthetic All-E astaxanthin (AST) (≥ 97 %) was from Thermo Scientific. Ethyl acetate (EtOAc, ≥99.7 %), absolute ethanol (EtOH, ≥99.8 %), methanol (MeOH≥99.8 %), sodium hydroxide (NaOH) pellets were purchased from Sigma-Aldrich and used as received. Ultrapure Milli-Q water, purified by a Millipore Milli-Q system (resistivity: 18.2 MΩ cm), was used to prepare aqueous solutions. LiI, I_2, $TiCl_4$, acetonitrile (ACN), valeronitrile (VN), all solvents used to prepare electrolyte solution, were from sigma Aldrich, Surlyn® gasket (Meltonix 1170–25) from Solaronix SA, platinum catalyst paste(PT1) from Greatcell Solar, fluorine-doped tin oxide (FTO) glass substrates, TiO_2 commercial paste (18NR-T), from Greatcell Solar.

2.2. Extraction of astaxanthin from the shrimp waste

The shrimp waste raw material, namely the cephalothorax from the red shrimp species *Aristaeomorpha foliacea* was obtained from a local fishing company. The material was stored frozen at −20 °C until use. The frozen cephalothoraxes are first homogenized using the Retsch Grindomix GM 200 at 10,000 rpm for 10 s and then dried to constant weight for 4 h in a fan oven at 50 °C. The dried material is further ground using the same instrument and settings, obtaining a fine powder. EtOAc and the shrimp cephalothorax powder are then mixed at a 5:1 v/w ratio and incubated for 20 min at room temperature under gentle shaking. After centrifugation at 5000*g* for 5 min, the supernatant is collected as "crude extract".

2.3. De-esterification of astaxanthin

De-esterification of astaxanthin in the shrimp crude extracts was carried out by means of a saponification procedure as follows: 100 μL of extract was mixed with 400 μL of MeOH containing 0.06 M NaOH, verifying that the pH reached a value around 10 as assessed by litmus

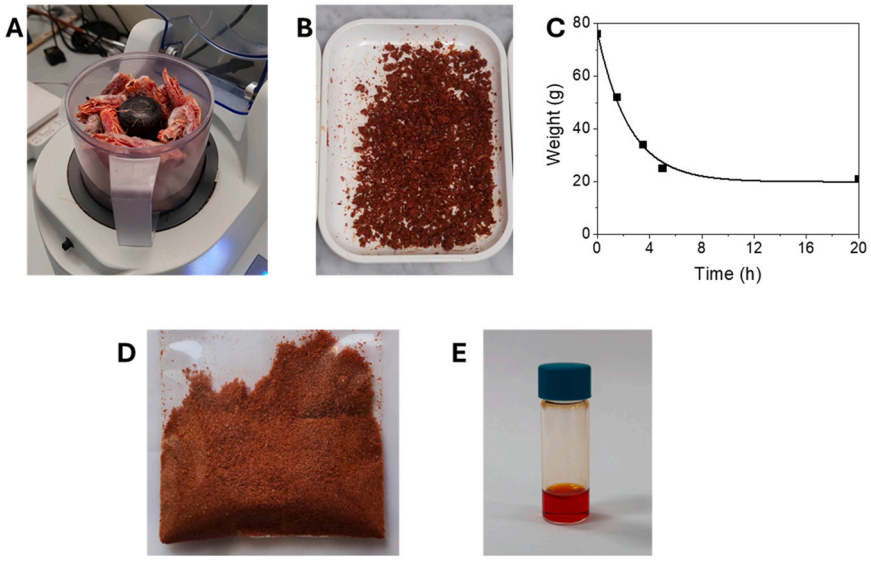

Fig. 1. Procedure used to obtain the astaxanthin-rich crude extracts from shrimp cephalothoraxes. A: frozen shrimp cephalothoraxes; B: coarse powder from the first milling; C: coarse powder desiccation curve; D: fine powder from the second milling; E: extract in EtOAc from the fine powder.

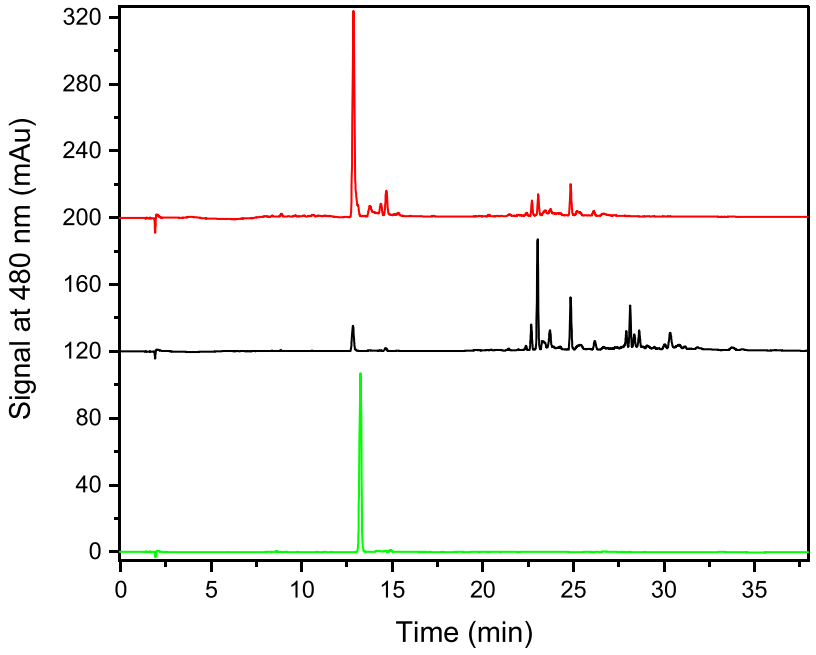

Fig. 2. Chromatographic profiles of AST standard (Green trace), EtOAc extract obtained from the shrimp cephalothoraxes powder after 20 min RT incubation at 5:1 v/w ratio and centrifugation (crude extract, black trace), and crude extract saponified with methanolic NaOH at ph 10 and neutralized with methanolic HCl (saponified extract, red trace).

paper. After incubation on ice for 3 h in the dark, the mixture was neutralized by adding 100 μL of MeOH containing 0.24 M HCl. Finally, the solution is dried under a gentle nitrogen stream and, if necessary, redissolved in the desired solvent for subsequent manipulations.

2.4. HPLC analysis of standard AST and shrimp cephalothoraxes extract

Chromatograms of AST were recorded using an Agilent 1100 series high-performance liquid chromatography (HPLC) system (Agilent Technologies, Palo Alto, CA) equipped with a binary pump (model G1312A), a solvent degasser (model G1379A) and a 1,024-element diode array detector (model G1315B), and controlled with the Agilent ChemStation software. The column was an Agilent Poroshell 120 SB-C18 (2.7 μm, 150 × 4.6 mm). MeOH-ACN-water (21:16.5:62.5, vol/vol/vol) containing 10 mM ammonium acetate was used as mobile phase A, while MeOH-ACN-EtOAc (50:20:30, vol/vol/vol) was used as mobile phase B. Elution was performed at a flow rate of 1 mL/min according to the following gradient program: 0 min, 20 % B; 0 –6 min 70 % B; 6 –24 min, 100 % B; 24 –36 min 100 % B [39].

2.5. Optical properties investigation

UV–visible (UV/Vis) spectra of the pigment solutions were recorded using a V-730 spectrophotometer (Jasco) with wavelength range 190–1100 nm. EtOH, the solvent used for the pigment resuspension, was used as blank. The optical properties of both the dye solution, to assess

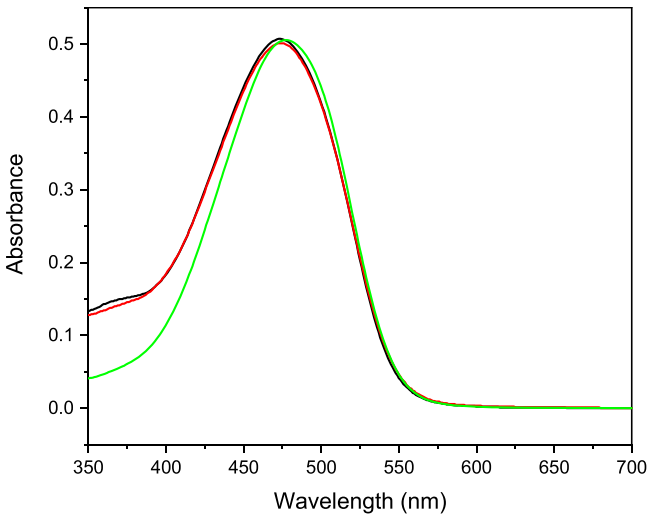

Fig. 3. Visible spectra of EtOAc solutions of AST standard (Green trace), crude extract (black trace) and saponified extract (red trace). all spectra have been normalized to 0.5 absorbance at the peak wavelength of 478 nm for AST standard and 474 nm for the crude and saponified extracts.

Table 1
Values of short-circuit photocurrent density (J_{SC}), open-circuit voltage (V_{OC}), fill factor (FF) and power conversion efficiency (PCE) related to different astaxanthin based sensitizing materials tested in this work in comparison to values obtained with other natural pigments. Average and standard deviation values are calculated over a set of 3 cells repeated three times.

Sample	J_{SC} (mA/cm^2)	V_{OC} (V)	FF	PCE (%)	Ref
crude shrimp extract	0.29 ± 0.03	0.46 ± 0.01	0.66 ± 0.03	0.09 ± 0.02	This work
saponified shrimp extract	2.12 ± 0.03	0.32 ± 0.03	0.45 ± 0.02	0.30 ± 0.02	This work
AST standard	2.36 ± 0.02	0.36 ± 0.03	0.54 ± 0.02	0.45 ± 0.01	This work
Astaxanthin source					
Bacterium *P. carotinifaciens*	2.86 ± 0.03	0.41 ± 0.05	0.3 ± 0.02	0.36 ± 0.04	[32]
Yeast *P. rhodozyma*	0.25 ± 0.02	0.36 ± 0.03	0.48 ± 0.01	0.04 ± 0.02	[32]
Microalga *H. pluvialis*	0.30 ± 0.01	0.29 ± 0.02	0.60 ± 0.01	0.05 ± 0.02	[32]
Other carotenoids					
tomato	0.51	0.14	0.37	0.03	[51]
Orange fruit	0.37	0.06	0.58	0.02	[51]
carrot	0.36	0.04	0.64	0.009	[51]
Crocin from gardenia fruit	0.45	0.58	0.60	0.16	[52]
crocetin from gardenia fruit	2.84	0.43	0.46	0.56	[52]

its absorption, and the photoanode, to evaluate the effective absorption of the dye on the semiconductor surface, were investigated.

2.6. DSSCs assembly and photoelectrochemical equipment

The DSSCs were developed following well-established procedures described in the literature and standardized methodologies [40–42]. The photoanode was prepared pre-treating a fluorine-doped tin oxide (FTO) glass substrate with aqueous $TiCl_4$ and, then, by applying a TiO_2 paste (commercial paste 18NR-T, Greatcell Solar) using the screen printing technique. The electrode was slowly heated in an airflow at 325 °C for 5 min, then at 375 °C for another 5 min, followed by 450 °C for 15 min, and finally at 550 °C for 30 min. Subsequently, the TiO_2 film was submerged in a $TiCl_4$ solution to form a top blocking layer. This process resulted in a mesoporous TiO_2 film with variable thickness, not exceeding 10 μm (a typical profile for natural dyes) and a particle size limited to 15 nm [43], as measured by profilometry, with an active area of 0.181 cm^2. Photoanodes were realized by soaking a TiO_2 film for 24 h in sensitizer solutions to allow dye adsorption.

To prepare the counter-electrodes, holes with a diameter of 1.5 mm were drilled into FTO-glass plates. These plates were then thoroughly washed with water and EtOH to eliminate any remaining glass powder or organic impurities. A transparent film of platinum catalyst (PT1, Greatcell Solar) was applied to the conductive side of the FTO-glass by using the doctor blade technique and heating the assembly at 550 °C for 30 min.

The photoanode and the platinum-based counter electrode were assembled in a sandwich configuration and sealed together using a thermopress (120 °C for 2 min) along with a hot melt Surlyn® gasket (Meltonix 1170–25, Solaronix SA). The electrolyte, AS8* (LiI 0.8 M, I_2 0.05 M in ACN:VN 85:15) was introduced into the cell via backfilling under vacuum, using a specialized syringe to eliminate any air inside, through a 1.5 mm diameter hole in the back of the cathode. Finally, the hole was sealed with an additional Surlyn® film and an epoxy resin was also applied as an additive sealant to prevent solvent leakage and to ensure greater temporal stability of the device [44].

A digital Keithley 236 multimeter connected to a PC and controlled by a homemade program was used to obtain the current–voltage (I-V) curves of the constructed devices. Simulated sunlight irradiation was provided by a LOT-Oriel solar simulator (Model LS0100–1000, 300 W Xe-arc lamp, powered by LSN251 power supply equipped with AM 1.5 filter, 100 mW/cm^2).

The DSSCs were connected to an Autolab Potentiostat/Galvanostat (Metrohm) equipped with a frequency response analyzer (FRA). EIS experiments were conducted over a frequency range of 100 kHz to 100 mHz at 0.45 V (0.01 Vrms) to compare the different performances. Data fitting for the extraction of equivalent circuit elements was carried out using NOVA software (Metrohm).

3. Results and discussion

3.1. Sample treatment and quanti-qualitative analysis

AST extraction was performed using a cost-effective and green methodology. The frozen shrimp cephalothoraxes, as obtained by the local fishing company, are wiped with paper to remove excess water and ground with a blade mill (Fig. 1A) to obtain a first course powder (Fig. 1B), then desiccated to constant weight in a fan oven at 50 °C. As can be seen from Fig. 1C, an acceptable degree of desiccation was obtained already within the first 5 h, hence this time was chosen to reduce the energy input of this step. After a second grinding step with the blade mill, the fine powder shown in Fig. 1D is obtained. Treatment with EtOAc in mild conditions (room temperature, 20 min, orbital shaking) enabled the extraction of the product shown in Fig. 1E. It is worthwhile to underline that EtOAc is a GRAS (Generally Recognized as Safe) solvent, approved by the U.S. Food and Drug Administration (FDA) and European Food Safety Authority (EFSA) as a pharmaceutical and food additive thanks to its low toxicity [45].

As is common for astaxanthin from natural sources, this carotenoid is mainly found in the mono- and diester forms, bound to fatty acid moieties of various lengths and degrees of saturation. Accordingly, Fig. 2 (black trace) shows that in our extracts free AST accounts only for a small fraction (~ 7 %, peak eluting after 12 min corresponding to that of authentic standard shown in Fig. 2 (green trace) while the mono-(~ 55 %, eluting in the interval 22–27 min) and diesters (~ 38 %, eluting in the interval 28–33 min) are the predominant forms.

From a quantitative standpoint, the AST yield obtained with these simple steps is among the highest reported in the literature [46], reaching the value of 670 μg/g, referred to the molecular weight of the free AST form. It is noteworthy that a similar yield can be obtained using

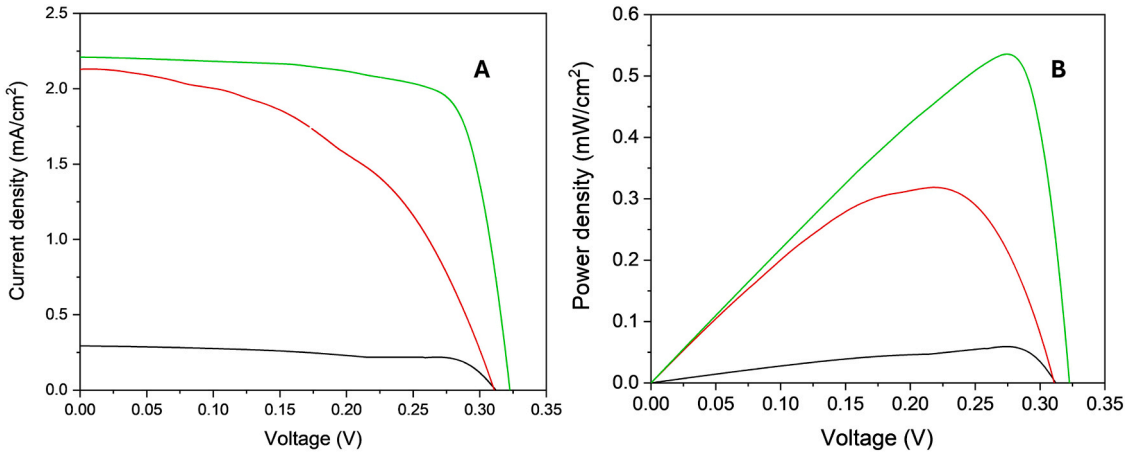

Fig. 4. A: IV and B: PV curves of devices sensitized by AST standard (Green line), crude extract from shrimp shells (black line) and saponified extract from shrimp shells (red line) acquired under simulated sunlight irradiation at 100 mW/cm^2.

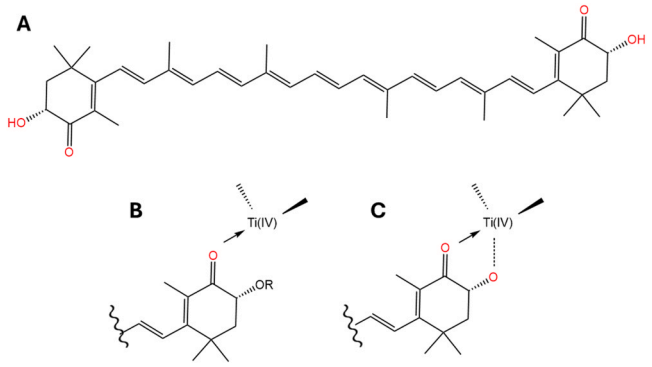

Fig. 5. A: AST standard structure; B: possible coordination configuration between esterified astaxanthin and TiO_2; C: possible coordination configuration between free astaxanthin and TiO_2.

the more energy-intensive lyophilization process to desiccate the shrimp cephalothoraxes.

De-esterification was also accomplished with minimal chemical manipulation, by diluting the extract with MeOH containing the calibrated amount of NaOH to maximize the de-esterification degree while minimizing degradation of astaxanthin. After neutralization and solvent evaporation, the sample is redissolved in EtOH and used to sensitize the DSSC. The chromatographic profile shown in Fig. 2 (red trace) confirms the presence of free all-E AST with minor amounts of monoester as well as isomerized forms (mainly 9-Z and 13-Z) whose peaks elute 1–2 mins after the main peak of the all-E form [47]. The astaxanthin standard is used as a reference to subsequently evaluate photovoltaic performance, and is hereafter referred to as the AST standard.

Visible spectra of the crude and saponified extracts along with that of the AST standard dissolved in EtOAc are shown in Fig. 3. The spectrum of standard astaxanthin presents a single peak at 475 nm according to literature data [48]. The spectra of the crude and saponified extracts are almost identical also featuring a single peak at 475 nm, further confirming that astaxanthin is the sole carotenoid found in the shrimps samples. The higher absorbance of both crude and saponified extracts compared to standard astaxanthin in the blue region is likely due to other lipophilic molecules co-extracted with the pigment.

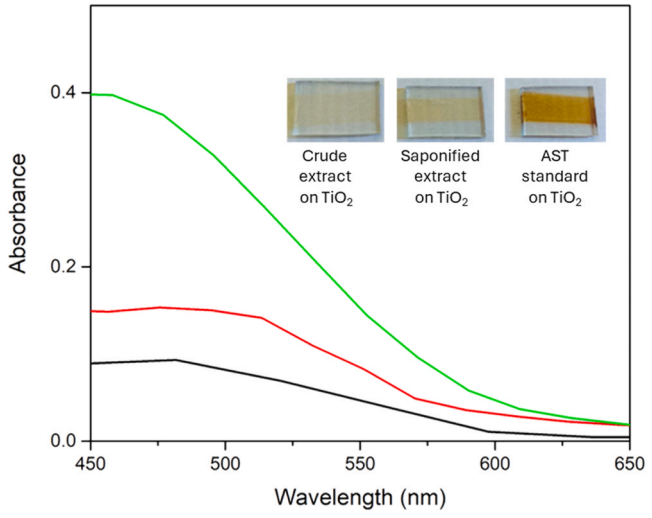

Fig. 6. Visible spectra of photoanodes made with AST standard (Green trace), crude extract from shrimp shells (black line) and saponified extract from shrimp shells (red line). inset: pictures of the three photoanodes.

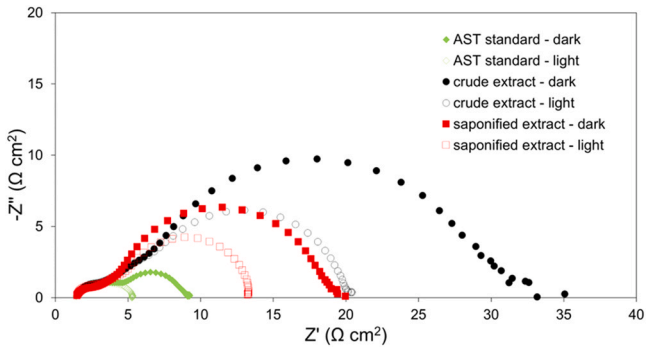

Fig. 7. EIS characterization of the DSSC sensitized with different materials.

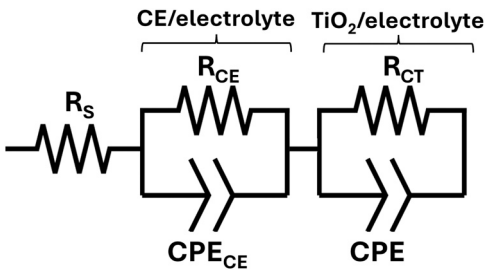

Fig. 8. Equivalent circuit model.

Table 2
Parameters of equivalent circuit model.

Sample	R_S (Ω cm^2)	R_{CE} (Ω cm^2)	CPE_{CE}		R_{CT} (Ω cm^2)	CPE	
			Y_1 (μS cm^{-2} s^n)	n_1		Y_1 (μS cm^{-2} s^n)	n_{22}
AST standard	1.5 ± 0.1	0.5 ± 0.1	4210.3 ± 0.1	0.61 ± 0.01	3.3 ± 0.1	976.3 ± 0.1	0.85 ± 0.01
crude extract	1.5 ± 0.1	2.5 ± 0.1	1985.3 ± 0.1	0.65 ± 0.01	16.4 ± 0.1	214 ± 0.1	0.88 ± 0.01
saponified extract	1.5 ± 0.1	2.5 ± 0.1	2204.5 ± 0.1	0.68 ± 0.01	9.2 ± 0.1	497.2 ± 0.1	0.81 ± 0.01

3.2. Photo electrochemical characterization

Unlike traditional silicon-based solar cells, DSSCs utilize a photosensitizing dye to absorb sunlight and generate electrical energy. At the core of a DSSC is a wide-bandgap semiconductor, typically titanium dioxide (TiO_2), which serves as the photoanode. The sensitizing dye, anchored to the surface of the TiO_2, absorbs photons from sunlight, leading to the excitation of electrons within the dye molecules [49]. These photoexcited electrons are rapidly injected into the conduction band of the TiO_2, from where they travel through the semiconductor to reach the anode electrode. The oxidized dye molecules are subsequently regenerated by a redox couple present in the electrolyte, commonly iodide/triiodide (I^-/I_3^-). This redox couple transfers electrons from the counter electrode back to the oxidized dye, completing the circuit and allowing continuous electron flow [50]. The counter electrode, often composed of platinum as catalyst, facilitates the reduction of the redox couple, thereby restoring the dye molecules to their ground state and enabling them to absorb additional photons.

The key performance metrics related to the functioning of DSSCs are:

- **Power Conversion Efficiency (PCE):** This is the most important figure of merit, representing the ratio of the electrical power output to the solar power input. It indicates the overall effectiveness of the DSSC in converting sunlight into electrical energy.

$$PCE\ (\%) = Voc \times Jsc \times FF$$

Where V_{oc} is the open-circuit voltage, J_{sc} is the short-circuit current density, FF is the fill factor.

- **Short-Circuit Current Density (J_{sc}):** This refers to the current generated per unit area of the DSSC when the cell is exposed to light, and the output terminals are shorted. It is a critical factor in determining the cell's ability to generate current.

$$J_{sc} = I_{sc}/A$$

Where I_{sc} is the short-circuit current and A is the active area of the DSSC.

- **Open-Circuit Voltage (V_{oc}):** This is the maximum voltage the DSSC can produce when there is no current flow (open circuit). A higher Voc indicates better performance in terms of energy conversion.
- **Fill Factor (FF):** The fill factor is the ratio of the maximum power output of the solar cell to the product of V_{oc} and J_{sc}. It reflects the quality of the DSSC and its ability to operate efficiently at maximum power.

These figures of merit, together with the corresponding formulas are used to calculate and evaluate the performance of DSSCs, focusing on their efficiency, current generation, and power output.

Three photoanodes were prepared by depositing the TiO_2 semiconductor onto FTO glass slides according to standard procedures and submerging them for 24 h in the dark into the following solutions: 1) dried crude extract redissolved in absolute EtOH; 2) dried saponified extract redissolved in absolute EtOH; 3) AST standard.

The DSSC devices were finally assembled, and relevant photoelectrochemical parameters were measured, under illumination at 100 mW/cm^2 and listed in Table 1, while the best I-V curves are reported in Fig. 4. Moreover, to better highlight the obtained result, the trends of the power density values as a function of voltage are shown in Fig. 4 B. To provide a clear and incisive understanding of the obtained values, the table also reports the photovoltaic parameters of devices in which AST-based pigments extracted from different microorganisms were used as sensitizers and compared with carotenoids of vegetable origin. The comparison shows that the only device exhibiting a higher efficiency value is the one in which crocetin was used, as it possesses R groups with a high number of hydroxyl groups in its molecular structure, allowing for better adhesion of the dye to the surface of the anode.

The device prepared with the dye extracted from the dried material without any chemical modification (crude extract) exhibited a very low efficiency value of 0.09 % (Table 1), consistent with the very low percentage of free astaxanthin present, as observed in the HPLC analysis. The device designed with the saponified extract showed a more photoactive behavior with a PCE of 0.30 %, while the best efficiency of 0.45 % was obtained with AST standard. The increase in efficiency from the crude to saponified extract is likely due to the higher availability of free -OH groups enhance the dye's binding affinity to the semiconductor surface. As a common feature of xanthophyll-type carotenoids, astaxanthin contains oxygen atoms, in this case under the form of two carbonyl and two hydroxylic groups, located in ortho position in the cyclic end groups at the extremities of the isoprenoid central core (Fig. 5A). A weak yet effective interaction between the esterified form of the AST and the TiO_2 surface is still expected, primarily via chemical adsorption through the only carbonyl functional group (Fig. 5B). However, upon de-esterification, the hydroxyl group becomes available, favoring a bidentate coordination mode, which becomes predominant, allowing a stronger and more stable interaction with the TiO_2 surface (Fig. 5C). This configuration is analogous to that proposed for anthocyanins, where chemical adsorption is widely accepted to occur due to the displacement of an OH^- counterion from the Ti (IV) site. The resulting coordination involves a proton donated by the anthocyanin moiety, forming a strong bidentate complex, in which the dye is prevalently in the quinonodial form [53,54].

In turn, the higher efficiency of the device made with AST standard is likely attributable to the greater amount of pigment that can be adsorbed onto the TiO_2 layer, which remains partially limited in the saponified extract due to the presence of co-extracted lipids and sterols. Indeed, the increasing amount of astaxanthin attached to the TiO_2 surface in the order AST standard> saponified extract > crude extract is clearly shown in the absorbance spectra of relevant photoanodes presented in Fig. 6. Nonetheless, the result obtained with the saponified extract represents an excellent outcome, considering the simple, rapid, and cost-effective method used to improve the performance of the material employed as the dye.

Also from an energetic standpoint, astaxanthin is expected to efficiently inject electrons into the TiO_2 layer as its LUMO level has been calculated to be −2.50 eV, above the energy of TiO_2 conduction band of −4.0 eV [55]. Conversely, the HOMO level, calculated to be −5.35 eV [55] or −5.03 eV [56] is below that of the I^-/I_3 redox couple of −4.80 eV, thus thermodynamically favoring dye regeneration.

For comparison, other carotene-type carotenoids such as β-carotene or lycopene, in addition to lacking suitable anchoring groups for TiO_2 grafting, have LUMO levels comparable to that of astaxanthin, but HOMO levels around −4.6 eV [57], which do not fulfill the thermodynamic requirement for dye regeneration. These considerations explain

why DSSC based on xanthophyll-type overperform those based on carotene-type, like lycopene [58].

In a relatively recent study [59], it was found that using astaxanthin as the sole sensitizer it was possible to fabricate a DSSC with 0.036 % efficiency, while using a crude extract from H*aematococcus pluvialis* resulted in an increased efficiency of 0.1 %, mainly attributed to a co-sensitizing effect from residual chlorophylls present in the un-purified extract.

3.3. EIS measurements

Fig. 7 displays the electrochemical impedance spectroscopy (EIS) data for dye-sensitized solar cells (DSSCs) using different materials: AST standard (green rhombuses, full for measurements in the dark and empty for measurements in the light), a crude shrimp extract (black circles full for measurements in the dark and empty for measurements in the light) and saponified shrimp extract (red squares, full for measurements in the dark and empty for measurements in the light). The graph plots the imaginary impedance (-Z") against the real impedance (Z′) to analyze charge transfer processes within the DSSC [60].

All EIS spectra feature the typical shape observed for DSSCs, consisting of two semicircles, one smaller at high frequencies, associated with kinetic processes at the Pt counter electrode of the solar cell, and one larger at high frequencies, associated with the photoelectrode and in particular with the charge transfer across the TiO_2/redox electrolyte interfaces [61]. The amplitude of this larger semicircle strictly depends on the sensitizer and in our case decreases in the order crude extract < saponified extract < AST standard, indicating a progressively more efficient charge transfer, which correlates well with the PCE values reported in Table 1. Moreover, all larger semicircles are in turn wider in the dark and narrower under illumination, due to light-enhanced charge transfer between the redox electrolyte and the TiO_2. The amplitude of the smaller semicircle is instead much less dependent on the nature of the sensitizer and/or illumination conditions and is mainly affected by the catalytic properties of the counter electrode.

Fig. 8 displays the equivalent circuit of the cell, which includes the following three elements connected in series [32,40,62]:

1) a resistance R_S given by the sum of the sheet resistance of FTO and the Pt counter electrode, and the resistance of the electrolyte
2) an element associated with the counter electrode/redox electrolyte interface represented by resistance R_{CE} in parallel with constant phase elements CPE_{CE}
3) an element associated with the TiO_2/redox electrolyte interface, represented by the resistance R_{CT} in parallel with a constant phase element CPE, in turn given by the sum of the surface-state capacitance of TiO_2 (C_{ss}), and the capacitance of the Helmholtz double layer (C_H).

Fitting the EIS data obtained under light condition for the three sensitizing materials to the above-described equivalent circuit model allowed to extract the values relevant to the different resistances and constant phase elements shown in Table 2, helping to quantitatively analyze the charge transfer processes within DSSC.

As expected, R_S has a small value, in line with its ohmic-contact nature, and is the same for all investigated systems. Also R_{CE} is small for all systems although slightly higher in the DSSCs sensitized with the shrimp extracts. The CPE_{CE} is moderately influenced by the sensitizing material, with larger values observed for the more efficient systems. Finally, R_{CT} and CPE are the parameters more directly related to the DSSC efficiency. R_{CT} is particularly low for the DSSC sensitized with standard astaxanthin and CPE exhibits the highest value. The comparison of R_{CT} for the crude and saponified extracts clearly shows how the saponification treatment substantially improves the DSSC performance, bringing it closer to that of the standard astaxanthin. The improvement shown by the saponified extract is consistent with the observed increase in the power conversion efficiency.

4. Conclusions

This study confirms the significant potential of astaxanthin extracted from shrimp waste as a natural photosensitizer for dye-sensitized solar cells (DSSCs), employing an environmentally friendly and economically viable approach. A cost-effective and rapid method was optimized to extract astaxanthin and subsequently convert it through de-esterification into a structure more suitable for interaction with the TiO_2 semiconductor surface.

The device sensitized with the de-esterified dye demonstrated enhanced photoactivity, as confirmed by electrochemical impedance spectroscopy (EIS), achieving a photoconversion efficiency (PCE) of 0.30 %. This represents a substantial improvement compared to the device fabricated with the crude, non-modified extract, which exhibited a very low efficiency of 0.09 %. Although still lower than 0.45 % obtained with the pure AST standard, these findings validate the effectiveness of the de-esterification process in improving the performance of shrimp-waste-derived astaxanthin as a sensitizer.

Beyond the promising photovoltaic results, this work demonstrates that it is possible to obtain high-quality, functional natural dyes through a methodology that avoids complex purification procedures, lyophilization, or extreme experimental conditions such as high energy input and ultra-high vacuum systems. The proposed route therefore offers a practical, accessible, and scalable alternative for sustainable photovoltaics, especially suited for decentralized applications or low-resource environments.

Moreover, the combination of efficient extraction, targeted de-esterification, and comprehensive characterization—through HPLC-DAD, UV–vis spectroscopy, current–voltage analysis, and EIS—confirms the scientific robustness of the approach and provides a repeatable framework for the future development of bio-derived DSSC sensitizers.

Looking forward, further studies will aim to reduce the impact of co-extracted lipophilic impurities, explore synergistic effects via co-sensitization with other natural pigments (e.g., chlorophylls or anthocyanins), evaluate alternative counter-electrode materials, and investigate the long-term stability of these bio-based devices under real-world solar irradiation.

CRediT authorship contribution statement

Federica Mancarella: Writing – original draft, Investigation, Formal analysis. **Francesco Milano:** Writing – review & editing, Writing – original draft, Visualization, Validation, Methodology, Investigation, Funding acquisition, Formal analysis, Data curation, Conceptualization. **Stefano Trocino:** Writing – original draft, Investigation, Formal analysis. **Ilaria Citro:** Writing – review & editing, Writing – original draft, Visualization, Validation, Supervision, Methodology, Investigation, Formal analysis, Data curation, Conceptualization. **Donatella Spadaro:** Writing – review & editing, Supervision, Resources, Project administration, Conceptualization. **Giuseppe Calogero:** Writing – original draft, Investigation, Formal analysis. **Livia Giotta:** Writing – original draft, Investigation, Formal analysis.

Declaration of Competing Interest

The authors declare that they have no known competing financial interests or personal relationships that could have appeared to influence the work reported in this paper.

Acknowledgements

We thank European Union (NextGeneration EU), through the MUR-PNRR project SAMOTHRACE — Sicilian Micro and Nano Technology

Research and Innovation Center (ECS00000022); PRIN Project 2022 n. 202293AX2L “Assessment of nano/microplastics impacts – PLASTACS”; FOE 2022 project FutuRaw - The raw materials of the future from non-critical, residual and renewable sources, NQSTI The National Quantum Science and Technology Institute (PE0000023). “ON Foods—Research and Innovation Network on Food and Nutrition Sustainability, Safety, and Security—Working ON Foods” (CUP B83C22004790001ONFOODS).

Data Availability

Data will be made available on request.

References

[1] J. Ramos, P. Ben, G. Patricia, A. García-Franco, E. Duque, Addressing the energy crisis: using microbes to make biofuels, Microb. Biotechnol. 15 (2022) 1026–1030, https://doi.org/10.1111/1751-7915.14050.
[2] J.C. Andrew, B. McLellan, T. Tezuka, Prioritizing mitigation efforts considering co-benefits, equity and energy justice: fossil fuel to renewable energy transition pathways, Appl. Energy (2018), https://doi.org/10.1016/J.APENERGY.2018.03.054.
[3] B. Hardin, H. Snaith, M. McGehee, The renaissance of dye-sensitized solar cells, Nat. Photonics 6 (2012) 162–169, https://doi.org/10.1038/nphoton.2012.22.
[4] M.K. Nazeeruddin, A. Kay, I. Rodicio, R. Humphry-Baker, E. Mueller, P. Liska, N. Vlachopoulos, M. Graetzel, Conversion of light to electricity by cis-X2bis(2,2′-bipyridyl-4,4′-dicarboxylate)ruthenium(II) charge-transfer sensitizers (X = Cl-, Br-, I-, CN-, and SCN-) on nanocrystalline titanium dioxide electrodes, JACS 115 (14) (1993) 6382–6390, https://doi.org/10.1021/ja00067a063.
[5] A.S. Polo, M.K. Itokazu, N.Y. Murakami Iha, Metal complex sensitizers in dye-sensitized solar cells, Coord. Chem. Rev. 248 (13) (2004) 1343–1361, https://doi.org/10.1016/j.ccr.2004.04.013.
[6] W. Yongzhen, Z. Weihong, S.M. Zakeeruddin, M. Grätzel, Insight into D-A-π-A structured sensitizers: a promising route to highly efficient and stable Dye-Sensitized solar cells, ACS Appl. Mater. Interfaces 7 (18) (2015) 9307–9318, https://doi.org/10.1021/acsami.5b02475.
[7] H. Choi, J.K. Lee, K. Song, S.O. Kang, J. Ko, Novel organic dyes containing bis-dimethylfluorenyl amino benzo[b]thiophene for highly efficient dye-sensitized solar cell, Tetrahedron 63 (15) (2007) 3115–3121, https://doi.org/10.1016/j.tet.2007.02.018.
[8] D. Zhang, N. Yamamoto, T. Yoshida, H. Minoura, Natural dye sensitized solar cells, Trans. Mater. Res. Soc. Jpn. 27 (4) (2002) 811–814.
[9] Q. Dai, J. Rabani, Unusually efficient photosensitization of nanocrystalline TiO2 films by pomegranate pigments in aqueous medium, N. J. Chem. 26 (4) (2002) 421–426, https://doi.org/10.1039/B108390B.
[10] G. Calogero, G.Di Marco, Red sicilian Orange and purple eggplant fruits as natural sensitizers for dye-sensitized solar cells, Sol. Energy Mater. Sol. Cells 92 (11) (2008) 1341–1346, https://doi.org/10.1016/j.solmat.2008.05.007.
[11] D. Spadaro, J. Barichello, I. Citro, G. Calogero, Environmentally friendly Water-Based electrolyte for Dye-Sensitized solar cells: future prospective and outlook, Solar 3 (2) (2023) 229–252, https://doi.org/10.3390/solar3020015.
[12] J. Barichello, P. Mariani, L. Vesce, D. Spadaro, I. Citro, F. Matteocci, A. Bartolotta, A. Di Carlo, G. Calogero, Bifacial dye-sensitized solar cells for indoor and outdoor renewable energy-based application, J. Mater. Chem. C. 12 (7) (2024) 2317–2349, https://doi.org/10.1039/D3TC03220E.
[13] K. Kenji, A. Yohei, T. Yano, K. Oya, J. Fujisawa, M. Hanaya, Highly-efficient dye-sensitized solar cells with collaborative sensitization by silyl-anchor and carboxy-anchor dyes, Chem. Commun. 51 (88) (2015) 15894–15897, https://doi.org/10.1039/c5cc06759f.
[14] O. Reiko, N. Shigeru, M. Morooka, M. Orihashi, S. Yusuke, K. Noda, High-performance dye-sensitized solar cell with a multiple dye system, Appl. Phys. Lett. 94 (2009) 73308, https://doi.org/10.1063/1.3086891.
[15] J. Cole, G. Pepe, K.A.B. Othman, B.C. Christopher, Cosensitization in Dye-Sensitized solar cells, Chem. Rev. (2019), https://doi.org/10.1021/acs.chemrev.8b00632.
[16] N.H. Abdul Manas, L.Y. Chong, Y.M. Tesfamariam, A. Zulkharnain, H. Mahmud, D. S. Abang Mahmod, S.F.Z. Mohamad Fuzi, N.I. Wan Azelee, Effects of oil substrate supplementation on production of prodigiosin by serratia nematodiphila for dye-sensitized solar cell, J. Biotechnol. 317 (2020) 16–26, https://doi.org/10.1016/j.jbiotec.2020.04.011.
[17] C. Silva, A. Santos, R. Salazar, C. Lamilla, B. Pavez, P. Meza, R. Hunter, L. Barrientos, Evaluation of dye sensitized solar cells based on a pigment obtained from antarctic streptomyces fildesensis, Sol. Energy 181 (2019) 379–385, https://doi.org/10.1016/j.solener.2019.01.035.
[18] P. Hernández-Velasco, I. Morales-Atilano, M. Rodríguez-Delgado, J.M. Rodríguez-Delgado, D. Luna-Moreno, F.G. Ávalos-Alanís, J.F. Villarreal-Chiu, Photoelectric evaluation of dye-sensitized solar cells based on prodigiosin pigment derived from serratia marcescens 11E, Dyes Pigments 177 (2020) 108278, https://doi.org/10.1016/j.dyepig.2020.108278.
[19] M.P. Narsing Rao, M. Xiao, W.-J. Li, Fungal and bacterial pigments: secondary metabolites with wide applications, Front. Microbiol 8 (2017), https://doi.org/10.3389/fmicb.2017.01113.
[20] A. Orona-Navar, I. Aguilar-Hernández, K.D.P. Nigam, A. Cerdán-Pasarán, N. Ornelas-Soto, Alternative sources of natural pigments for dye-sensitized solar cells: algae, Cyanobacteria, bacteria, archaea and fungi, J. Biotechnol. 332 (2021) 29–53, https://doi.org/10.1016/j.jbiotec.2021.03.013.
[21] H.A. Maddah, V. Berry, S.K. Behura, Biomolecular photosensitizers for dye-sensitized solar cells: recent developments and critical insights, Renew. Sustain. Energy Rev. 121 (2020) 109678, https://doi.org/10.1016/j.rser.2019.109678.
[22] A. Kay, M. Graetzel, Artificial photosynthesis. 1. photosensitization of titania solar cells with chlorophyll derivatives and related natural porphyrins, J. Phys. Chem. 97 (23) (1993) 6272–6277, https://doi.org/10.1021/j100125a029.
[23] N.J. Cherepy, G.P. Smestad, M. Grätzel, J.Z. Zhang, Ultrafast electron injection: implications for a photoelectrochemical cell utilizing an anthocyanin Dye-Sensitized TiO2 nanocrystalline electrode, J. Phys. Chem. B 101 (45) (1997) 9342–9351, https://doi.org/10.1021/jp972197w.
[24] K. Prajapat, U. Mahajan, M. Dhonde, K. Sahu, P. Sakthivel, S. Vyas, P.M. Shirage, Anthocyanin-sensitized Cu-doped TiO2 nanoparticles for efficient and sustainable DSSCs, Mater. Adv. 6 (7) (2025) 2371–2384, https://doi.org/10.1039/D4MA01297F.
[25] C. Sandquist, J.L. McHale, Improved efficiency of betanin-based dye-sensitized solar cells, J. Photochem. Photobiol. A Chem. 221 (1) (2011) 90–97, https://doi.org/10.1016/j.jphotochem.2011.04.030.
[26] G.G. Asfaw, N.E. Benti, M.A. Desta, Y.S. Mekonnen, Design and fabrication of TiO2-based dye sensitized solar cells using plant-derived organic dyes, AIP Adv. 13 (7) (2023) 075120, https://doi.org/10.1063/5.0153639.
[27] K. Prajapat, U. Mahajan, K. Sahu, M. Dhonde, P.M. Shirage, The evolution of natural Dye-Sensitized solar cells: current advances and future outlook, Sol. Energy 284 (2024) 113081, https://doi.org/10.1016/j.solener.2024.113081.
[28] A.M. Ammar, H.S.H. Mohamed, M.M.K. Yousef, G.M. Abdel-Hafez, A.S. Hassanien, A.S.G. Khalil, Dye-Sensitized solar cells (DSSCs) based on extracted natural dyes, J. Nanomater. 2019 (1) (2019) 1867271, https://doi.org/10.1155/2019/1867271.
[29] G. Calogero, A. Bartolotta, G. Di Marco, A. Di Carlo, F. Bonaccorso, Vegetable-based dye-sensitized solar cells, Chem. Soc. Rev. 44 (10) (2015) 3244–3294, https://doi.org/10.1039/C4CS00309H.
[30] D. Zhou, Z. Fei, G. Liu, Y. Jiang, W. Jiang, C.S.K. Lin, W. Zhang, F. Xin, M. Jiang, The bioproduction of astaxanthin: a comprehensive review on the microbial synthesis and downstream extraction, Biotechnol. Adv. 74 (2024) 108392, https://doi.org/10.1016/j.biotechadv.2024.108392.
[31] E. Arunkumar, S. Bhuvaneswari, C.V. Anuradha, An intervention study in obese mice with astaxanthin, a marine carotenoid – effects on insulin signaling and pro-inflammatory cytokines, Food Funct. 3 (2) (2012) 120–126, https://doi.org/10.1039/C1FO10161G.
[32] A. Tropea, D. Spadaro, I. Citro, M. Lanza, S. Trocino, R.L. Tella, D. Giuffrida, C. U. Mussagy, L. Mondello, G. Calogero, The influence of microbial sources on astaxanthin implementation as sensitizer in dye sensitized solar cells (DSSCs), J. Photochem. Photobiol. A Chem. 461 (2025) 116174, https://doi.org/10.1016/j.jphotochem.2024.116174.
[33] L. Wang, J. Hu, W. Lv, W. Lu, D. Pei, Y. Lv, W. Wang, M. Zhang, R. Ding, M. Lv, Optimized extraction of astaxanthin from shrimp shells treated by biological enzyme and its separation and purification using macroporous resin, Food Chem. 363 (2021) 130369, https://doi.org/10.1016/j.foodchem.2021.130369.
[34] M. Gharibzadeh, S. Osfouri, A. Jamekhorshid, S.A. Jafari, Microbial chitin extraction and characterization from Green tiger shrimp waste: a comparative study of culture mediums along with bioprocess optimization, Int. J. Biol. Macromol. 242 (2023) 125213, https://doi.org/10.1016/j.ijbiomac.2023.125213.
[35] J. Gómez-Estaca, M.M. Calvo, I. Álvarez-Acero, P. Montero, M.C. Gómez-Guillén, Characterization and storage stability of astaxanthin esters, fatty acid profile and α-tocopherol of lipid extract from shrimp (L. vannamei) waste with potential applications as food ingredient, Food Chem. 216 (2017) 37–44, https://doi.org/10.1016/j.foodchem.2016.08.016.
[36] X. Mao, N. Guo, J. Sun, C. Xue, Comprehensive utilization of shrimp waste based on biotechnological methods: a review, J. Clean. Prod. 143 (2017) 814–823, https://doi.org/10.1016/j.jclepro.2016.12.042.
[37] H. Yang, G. Gözaydın, R.R. Nasaruddin, J.R.G. Har, X. Chen, X. Wang, N. Yan, Toward the shell biorefinery: processing crustacean shell waste using hot water and carbonic acid, ACS Sustain. Chem. Eng. 7 (5) (2019) 5532–5542, https://doi.org/10.1021/acssuschemeng.8b06853.
[38] F. Mancarella, F. Milano, P. Semeraro, V.D. Leo, F. Messa, S. Perrone, A. Salomone, M. Durante, M.S. Lenucci, M.D. Benedictis, A. Santino, L. Giotta, L. Valli, Binary mixtures of menthol and alkanoic acids as Green solvents for efficient astaxanthin recovery from aristaeomorpha foliacea shrimp shells, Sep. Purif. Technol. (2025) 133261, https://doi.org/10.1016/j.seppur.2025.133261.
[39] E.Graham Joel, A.Bryant Donald, The biosynthetic pathway for synechoxanthin, an aromatic carotenoid synthesized by the euryhaline, unicellular cyanobacterium synechococcus sp. Strain PCC 7002, J. Bacteriol. 190 (24) (2008) 7966–7974, https://doi.org/10.1128/jb.00985-08.
[40] A. Tropea, D. Spadaro, S. Trocino, D. Giuffrida, T.M.G. Salerno, J.P. Ruiz-Sanchez, J. Montañez, L. Morales-Oyervides, L. Dufossé, L. Mondello, G. Calogero, Development of dye-sensitized solar cells using pigment extracts produced by talaromyces atroroseus GH2, Photochem. Photobiol. Sci. 23 (5) (2024) 941–955, https://doi.org/10.1007/s43630-024-00566-x.
[41] A. Bartolotta, G. Calogero, Chapter four - Dye-sensitized solar cells: from synthetic dyes to natural pigments, in: F. Enrichi, G.C. Righini (Eds.), Solar Cells and Light Management, Elsevier, 2020, pp. 107–161, https://doi.org/10.1016/B978-0-08-102762-2.00004-5.
[42] G. Calogero, J. Barichello, I. Citro, P. Mariani, L. Vesce, A. Bartolotta, A. Di Carlo, G. Di Marco, Photoelectrochemical and spectrophotometric studies on dye-

sensitized solar cells (DSCs) and stable modules (DSCMs) based on natural apocarotenoids pigments, Dyes Pigments 155 (2018) 75–83, https://doi.org/10.1016/j.dyepig.2018.03.021.
[43] F. Bella, C. Gerbaldi, C. Barolo, M. Grätzel, Aqueous dye-sensitized solar cells, Chem. Soc. Rev. 44 (11) (2015) 3431–3473, https://doi.org/10.1039/C4CS00456F.
[44] G. Calogero, I. Citro, C. Crupi, G. Carini, D. Arigò, G. Spinella, A. Bartolotta, G. Di Marco, Absorption spectra, thermal analysis, photoelectrochemical characterization and stability test of vegetable-based dye-sensitized solar cells, Opt. Mater. 88 (2019) 24–29, https://doi.org/10.1016/j.optmat.2018.11.005.
[45] D. Villanueva-Bermejo, G. Reglero, T. Fornari, Recent advances in the processing of Green tea biomolecules using ethyl lactate. A review, Trends Food Sci. Technol. 62 (2017) 1–12, https://doi.org/10.1016/j.tifs.2016.12.009.
[46] C. Irna, I. Jaswir, R. Othman, D.N. Jimat, Comparison between High-Pressure processing and chemical extraction: astaxanthin yield from six species of shrimp carapace, J. Diet. Suppl. 15 (6) (2018) 805–813, https://doi.org/10.1080/19390211.2017.1387885.
[47] C. Yang, L. Zhang, H. Zhang, Q. Sun, R. Liu, J. Li, L. Wu, R. Tsao, Rapid and efficient conversion of All-E-astaxanthin to 9Z- and 13Z-Isomers and assessment of their stability and antioxidant activities, J. Agric. Food Chem. 65 (4) (2017) 818–826, https://doi.org/10.1021/acs.jafc.6b04962.
[48] N.W. Withers, E.R. Cox, R. Tomas, F.T. Haxo, Pigments of the dinoflagellate peridinium balticum and its photosynthetic endosymbiont, J. Phycol. 13 (4) (1977) 354–358, https://doi.org/10.1111/j.1529-8817.1977.tb02941.x.
[49] M. Ye, X. Wen, W. Mengye, I. James, N. Zhang, L. Changjian, L. Zhiqun, Recent advances in dye-sensitized solar cells: from photoanodes, sensitizers and electrolytes to counter electrodes, Mater. Today 18 (2015) 155–162, https://doi.org/10.1016/J.MATTOD.2014.09.001.
[50] L. Kavan, Electrochemistry and dye-sensitized solar cells, Curr. Opin. Electrochem. 2 (2017) 88–96, https://doi.org/10.1016/J.COELEC.2017.03.008.
[51] A. Supriyanto, F. Nurosyid, A.H. Ahliha, Carotenoid pigment as sensitizers for applications of dye-sensitized solar cell (DSSC), IOP Conference Series Materials Science Engineering 432 (1) (2018) 012060, https://doi.org/10.1088/1757-899X/432/1/012060.
[52] E. Yamazaki, M. Murayama, N. Nishikawa, N. Hashimoto, M. Shoyama, O. Kurita, Utilization of natural carotenoids as photosensitizers for dye-sensitized solar cells, Sol. Energy 81 (4) (2007) 512–516, https://doi.org/10.1016/j.solener.2006.08.003.
[53] P. Luo, H. Niu, G. Zheng, X. Bai, M. Zhang, W. Wang, From salmon pink to blue natural sensitizers for solar cells: canna indica L., salvia splendens, cowberry and solanum nigrum l, Spectrochim. Acta Part A Mol. Biomol. Spectrosc. 74 (4) (2009) 936–942, https://doi.org/10.1016/j.saa.2009.08.039.
[54] R. Ramamoorthy, K. Karthika, A. Maggie Dayana, G. Maheswari, V. Eswaramoorthi, N. Pavithra, S. Anandan, R. Victor Williams, Reduced graphene oxide embedded titanium dioxide nanocomposite as novel photoanode material in natural dye-sensitized solar cells, Journal Materials Science Materials Electronics 28 (18) (2017) 13678–13689, https://doi.org/10.1007/s10854-017-7211-0.
[55] J. Huang, H. Yu, The high-performance organic solar cells with an improved efficiency and stability by incorporating environmental biomaterial astaxanthin, Electrochim. Acta 439 (2023) 141684, https://doi.org/10.1016/j.electacta.2022.141684.
[56] S. Wibowo, S. Widyarti, A. Sabarudin, D.W. Soeatmadji, S.B. Sumitro, DFT and molecular dynamics studies of astaxanthin-metal ions (Cu2+ and Zn2+) complex to prevent glycated human serum albumin from possible unfolding, Heliyon 7 (3) (2021) e06548, https://doi.org/10.1016/j.heliyon.2021.e06548.
[57] M. Flores-Hidalgo, F. Torres-Rivas, J.M. Bensojo, M. Escobedo-Bretado, D. Glossman-Mitnik, D. Barraza-Jimenez, Electronic structure of carotenoids in natural and artificial photosynthesis, in: J.C. Dragan, S.N. Goran (Eds.), Carotenoids, IntechOpen, Rijeka, 2017, https://doi.org/10.5772/67636.
[58] D.R. Shinde, P.S. Tambade, K.M. Gadave, K.S. Pawar, M. Naushad, H.M. Pathan, Dye-sensitised solar cells with a naturally occurring pigment lycopene as a photosensitiser for zirconium dioxide: an experimental and theoretical study, Journal Materials Science Materials Electronics 28 (15) (2017) 11311–11316, https://doi.org/10.1007/s10854-017-6923-5.
[59] A. Orona-Navar, I. Aguilar-Hernández, A. Cerdán-Pasarán, T. López-Luke, M. Rodríguez-Delgado, D.L. Cárdenas-Chávez, E. Cepeda-Pérez, N. Ornelas-Soto, Astaxanthin from haematococcus pluvialis as a natural photosensitizer for dye-sensitized solar cell, Algal Res. 26 (2017) 15–24, https://doi.org/10.1016/j.algal.2017.06.027.
[60] L. Bay, K. West, An equivalent circuit approach to the modelling of the dynamics of dye sensitized solar cells, Sol. Energy Mater. Sol. Cells 87 (1) (2005) 613–628, https://doi.org/10.1016/j.solmat.2004.08.022.
[61] J. van de Lagemaat, N.G. Park, A.J. Frank, Influence of electrical potential distribution, charge transport, and recombination on the photopotential and photocurrent conversion efficiency of Dye-Sensitized nanocrystalline TiO2 solar cells: a study by electrical impedance and optical modulation techniques, J. Phys. Chem. B 104 (9) (2000) 2044–2052, https://doi.org/10.1021/jp993172v.
[62] D. Spadaro, A. Tropea, I. Citro, S. Trocino, D. Giuffrida, F. Rigano, L. Morales-Oyervides, T. Brinkhoff, T. Tiso, L. Dufossé, G. Calogero, L. Mondello, Development of innovative dye sensitized solar cells (DSSCs) based on co-sensitization of natural microbial pigments, Dyes Pigments 229 (2024) 112311, https://doi.org/10.1016/j.dyepig.2024.112311.